Design of Instrumentation for Metabolic Monitoring of the Adélie Penguin

A thesis presented in partial fulfillment of
the requirements for the degree of
Master of Science
in Physics at
Massey University

by

Paul Stephen Ryland

December 2000

Abstract

The motivating question for the work described in this thesis was "How does the Adélie penguin cope with cold?" It was reasoned that the time-scale of temperature changes in Antarctica precluded all but metabolic and physiological responses. To determine these, a system capable of measuring and recording these biological variables in the penguins natural environment, was designed.

A device, based on the principles of near infrared spectroscopy, was developed that could measure the relative oxygen saturation of haemoglobin and the reduction state of cytochrome oxidase as well as heart rate and blood volume. The completed device was housed in a black, waterproof, plastic container, measuring 65mm x 92mm x 25mm and weighing 132.7g.

Co-ordination of measurements was achieved with operating system-like control software implemented in Motorola HC11 assembly code. Synchronous detection was used for signal acquisition and a pulse algorithm, implemented in assembly code, allowed real time pulse measurement from the input signals. Programs were written in Matlab and C++ to investigate the characteristics and limits of these techniques.

Preliminary testing of the device on human subjects successfully showed changes in metabolic state as a result of physical activity. The results of field testing on Adélie penguins were unable to answer the original question due to a number of physical factors. However, the success of human trials suggests that, with modification and improvement, the device has potential as a valuable research instrument, applicable to a variety of other species.

Acknowledgements

I would like to express my sincere gratitude to the following people whose contribution and assistance were invaluable to me and to the completion of this thesis. I have gained an enormous amount from their skills and expertise and know that the knowledge and experience gained will continue to be valuable in the future. Particular thanks go to my supervisor, Dr. Simon Brown, for his considerable contribution and guidance throughout the many aspects of the project. In areas ranging from remedial biology, lab work, field work, presentations, CV writing, grant applications and thesis proofing, his enthusiasm for the project and encouragement have been exceptional. I also wish to thank my co-supervisor, Associate Professor Robert O'Driscoll for the introduction to this project and whose extensive electronics expertise guided me in solving some of my most taxing hardware and software problems.

I gratefully thank the electronics guru, Robin Dykstra, for directing my circuit design efforts, providing development equipment and manuals, component advise, his stringent, NASA approved circuit-board-layout quality control and good friendship. Thanks also to Peter Lewis who helped select and order numerous electronic components, made an exceptional contribution during the time critical construction phase allowing deadlines to be met and even provided reading material for the quiet times in Antarctica. Also from the electronics workshop, I wish to thank Udo von Mulert for allowing the extensive use of the workshop facilities after hours and on weekends, and Keith Whitehead for his advise and ideas on numerous aspects of the project.

For her help in Antarctica, expert penguin handling skills and easy going personality I would like to thank Yvette Cottam. I also wish to express my gratitude to Antarctica New Zealand for their approval of the work in Antarctica with the Adélie penguin and to Massey University for the opportunity to work on this project. I thank Massey University for the approval of my Institute of Fundamental Sciences Graduate Research Fund application amounting in $1731 towards purchase of equipment and related expenses.

Particular thanks to John Pedley for his help with the use of the ECG to test the second prototype and for the loan of the exer-cycle used to test the third prototype. I would also like to recognize the many test subjects who exerted themselves in the name of science, in particular, to Jane Shierlaw whose high quality data made it to print. I would also like to thank Jane for her veterinary advice as well as thesis writing comments and ideas. Finally, I would especially like to thank Mark Hunter for the very many coffees, countless ridiculously late nights and for being someone available to discuss the more subtle points of thesis writing (some of which were relevant).

Contents

List of Figures

Chapter 1

Introduction

1.1 The problem

For the Adélie penguin (*Pygoscelis adélie*) of Antarctica there exists an intriguing biological paradox. As for any animal living in this environment, adaptation to cold and the regulation of body temperature is of primary importance. During breeding however, the Adélie penguins exhibit behaviour that seems to defy these thermal demands. For periods lasting as long as two weeks [1] they remain on their nests vigilantly guarding their eggs. During this time they fast, exhibit minimal muscular activity and no behavioural activities such as huddling. Fasting results in a reduction of resting metabolic rate thereby conserving energy. Contrary to this, an adaptive response to cold is to increase metabolic rate, producing heat from food or body fat reserves. As the penguins are fasting, this increase in metabolic rate results in the depletion of the bird's insulating body fat layer, further increasing the need for heat generation. As thermogenesis does not occur significantly by other means there seem to be conflicting metabolic demands and the question arises, 'How does the Adélie penguin cope in this environment?'

1.2 Measurement

An increase in metabolic rate implies an increase in the demand for oxygen. Processes that exhibit a response to changes in metabolic rate are the transport of oxygen via haemoglobin and the oxidation of substrates within cells by oxidative phosphorylation. Two proteins involved in these processes, haemoglobin (Hb) and cytochrome oxidase (COX), exhibit changes in their spectral characteristics depending on their oxygenation state. These spectra can be observed *in vivo* using near-infrared (NIR) spectroscopy, a technique that has been employed successfully with the human foetus, neonate and adult [2].

Oxidised and reduced haemoglobin and cytochrome oxidase exist in equilibrium in blood and in the mitochondria of cells respectively (1.1 and 1.2). The equilibrium concentrations for each of these give information about the supply and demand for oxygen at the beginning and end of the metabolic process.

$$Hb + O_2 \rightleftharpoons HbO_2 \qquad (1.1)$$

$$COX + O_2 \rightleftharpoons COXO_2 \qquad (1.2)$$

Haemoglobin, oxygen and oxyhaemoglobin are transported throughout the body via blood vessels (figure 1.1). A concentration gradient between the blood and the cell causes oxygen to diffuse through the wall of the blood vessel into the cell. Higher concentrations of oxyhaemoglobin observed in the blood imply that the supply of oxygen is greater than the demand due to decreased respiration or reduced metabolic

rate. If oxyhaemoglobin concentrations decrease, then oxygen consumption is greater than the demand as a result of increased respiration or higher metabolic rate.

Oxygen is consumed within the cell during the last stage of oxidative phosphorylation. Within the cell, sugar is broken down into a smaller molecule called pyruvate that is oxidised within the mitochondria to produce the waste products; carbon dioxide and water. This final reaction is catalysed by cytochrome oxidase that exists in equilibrium with oxygen in the mitochondrial membrane. If high levels of oxidised cytochrome oxidase are observed, this indicates that the rate of sugar metabolism is slow and, conversely, highly reduced cytochrome oxidase indicates an increased metabolic rate.

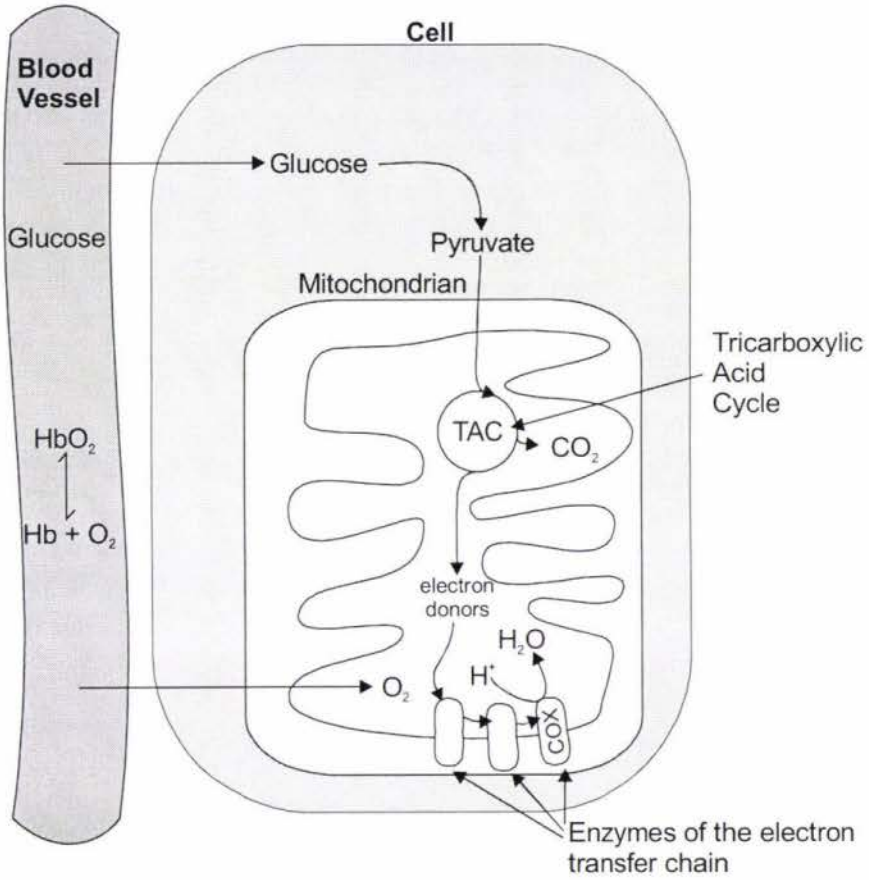

Figure 1.1: The metabolism of sugar with the cell. Oxygen exists in equilibrium with two proteins, haemoglobin and cytochrome oxidase, in blood and in the mitochondria within cells respectively. The spectral characteristics of these two proteins depend on the relative concentrations of their oxidised and reduced forms. Changes in these spectra give information about the rate of oxygen metabolism.

By developing a device capable of making oxygen saturation measurements along with pulse and temperature measurements a correlation may be observed between the environmental temperature and biological responses of the penguin. Such a device must be portable, small and lightweight so as not to inhibit the normal activities of the bird or cause stress resulting in unrealistic data. NIR spectroscopy, a non-invasive technique, is ideally suited to this problem and the development of such an instrument would allow changes in the relative oxygen saturation to be observed with minimal impact on the penguin.

1.3 Background – The Adélie Environment

Antarctica, and its surrounding oceans, form one of the most extreme, and yet habitable, environments on earth. All species that live and breed in this southern polar region face the same survival issue: the adaptation to cold and maintenance of body temperature. Each animal that lives in or visits this environment exhibits biological or behavioural adaptations that enable it to combat the extreme cold such as increased body fat, thicker skin/feather layers or group huddling behaviour. Adélie penguins spend eight months of the year living and foraging off the pack ice that forms where the polar ice cap meets the southern ocean. The birds move with the pack ice that advances and recedes seasonally, covering a distance of over 1300km [3]. Starting around mid October, the Adélie penguins make a trek, often travelling 80km or more inland, to their annual breeding sites located on the shores of the Antarctic mainland or on many of the Antarctic islands. Some nesting colonies can number in the tens of thousands and on Ross Island (figure 1.2), where there are six colonies [4], a major nesting site of approximately 60,000 Adélie penguins is located at Cape Bird (Barton, K. J., personal communication).

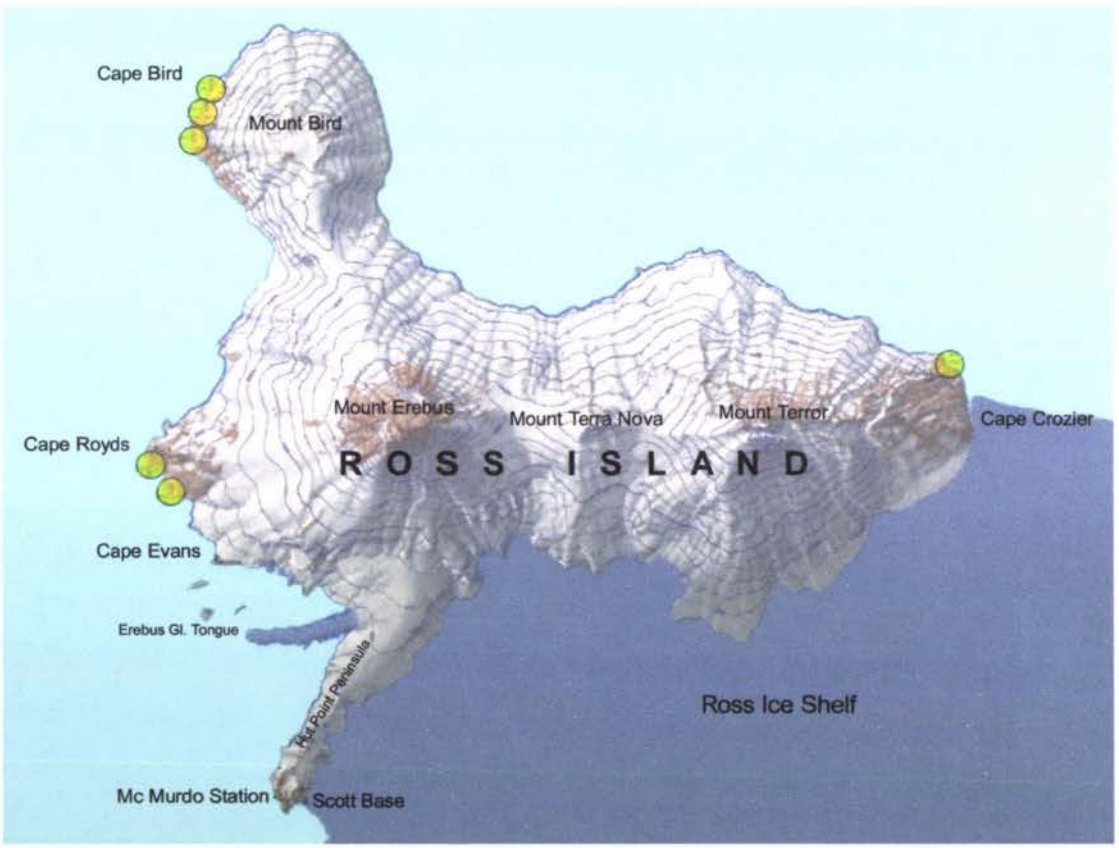

Figure 1.2: Ross Island and breeding colonies of the Adélie penguin. The Adélie penguin rookeries are indicated in yellow. At Cape Bird an Adélie colony numbering approximately 60,000 forms every year from early November to mid January.

Upon arrival at the nesting site the males, who arrive earlier than the females, begin constructing nests. Open windswept mounds and ridges are the usual location for the nests as these snow-free areas are all that is available when the Adélies arrive in early spring. The Adélies collect stones ranging in size from 1cm to 5cm and place them around the edge of a depression in the ground forming a doughnut shaped wall on which the penguin sits (figure 1.3).

Figure 1.3: An Adélie penguin upon its nest of pebbles. The nest consists of pebbles between 1cm and 5cm in diameter arranged around a depression in the ground. Nests are constructed on snow-free mounds to avoid streams and puddles when surrounding snow and ice melts. Unfortunately these regions are also exposed to harsh weather conditions.

This choice of nest location has both advantages and disadvantages. As spring turns to summer the surrounding snow and ice melts forming streams and puddles that these raised regions avoid. Unfortunately, these raised areas are also exposed to wind and during the early stages of brooding the Adélies have to contend with harsh spring weather conditions. In the early weeks of November the male Adélies may endure temperature fluctuations of approximately 20°C brought on by increased wind chill due to blowing snow. More surprisingly, on still days the Adélie is faced with a heat dissipation problem due to the zero humidity of Antarctic air. Under constant sunlight, local air temperatures can rise well above zero and on these 'hot' days nesting Adélies will lie with flippers and feet outstretched in an attempt to dissipate heat. For birds without eggs to protect, the overheating problem is solved by lying in or eating snow.

The total incubation period for Adélie eggs is between 33 and 39 days and, in 88% of cases, the male incubates the eggs for the first 14 days. During this time he fasts [1]. Since there are few other options, thermo-regulation must occur on a systemic level through variation in heart rate, metabolic rate, respiratory rate and vasoconstriction. The goal of this thesis was to develop a system capable of measuring these responses and provide an insight into the homeostatic mechanisms of the Adélie penguin.

1.4 Technology

The basic requirements of NIR spectroscopy are a monochromatic light source in the red and infrared region of the electromagnetic spectrum and a photo-detector sensitive enough to respond to the subtle changes in scattered light intensity. The options considered for light sources were either laser diodes or LEDs as other sources were impracticably large. An attractive aspect of using laser diodes includes increased incident illumination and temporal coherence. However, temperature instability, cost, power consumption and the lack of availability over a range of frequencies prohibited their use. Recent development in LED technology has seen a dramatic increase in the intensity and range of available frequencies. Combined with their cost, weight, power consumption and acceptable coherence (typical linewidth of 20nm), they were selected as the most suitable light sources for the device.

The options available as detectors included photodiodes of varying areas and construction or a photo-multiplier. The later was eliminated for cost and size reasons and of the photodiodes, a large area ($7.5mm^2$) silicon detector was selected as its cost, sensitive range and temperature stability made it favourable. Other possibilities were hybrid photo-detector/preamplifier devices, however their expense precluded their use.

Basic improvement to a NIR spectroscopic system is achieved by either increasing the intensity of the incident light or increasing the effective sensitivity of the detector. The factors considered when designing the device also included cost, weight, size, temperature stability and power consumption.

1.5 Measurement Principles

1.5.1 NEAR INFRARED SPECTROSCOPY

The biological and medical value of near infrared spectroscopy arises from the relative transparency of tissue to light in the red and near infrared regions of the electromagnetic spectrum and the presence of two natural chromophores that exhibit oxygenation dependent absorption at these wavelengths (figure 1.4). These chromophores are haemoglobin, which is present in red blood cells and is therefore an indicator of blood oxygenation, and cytochrome oxidase, which is the terminal enzyme in the mitochondrial electron transfer chain and therefore an indicator of tissue oxygenation [5]. The goal of NIR spectroscopy is to obtain absolute quantitative absorption spectra through observed changes in detected scattered light. However, differences from subject to subject in physical attributes such as skin opacity, skin thickness, blood circulation and temperature preclude single wavelength measurements due to an inability to calibrate the system. Using double wavelength techniques similar to that used by Shiga [6] and Mendelson [7], qualitative oxygen saturation data are obtained through normalisation of the absorbance data.

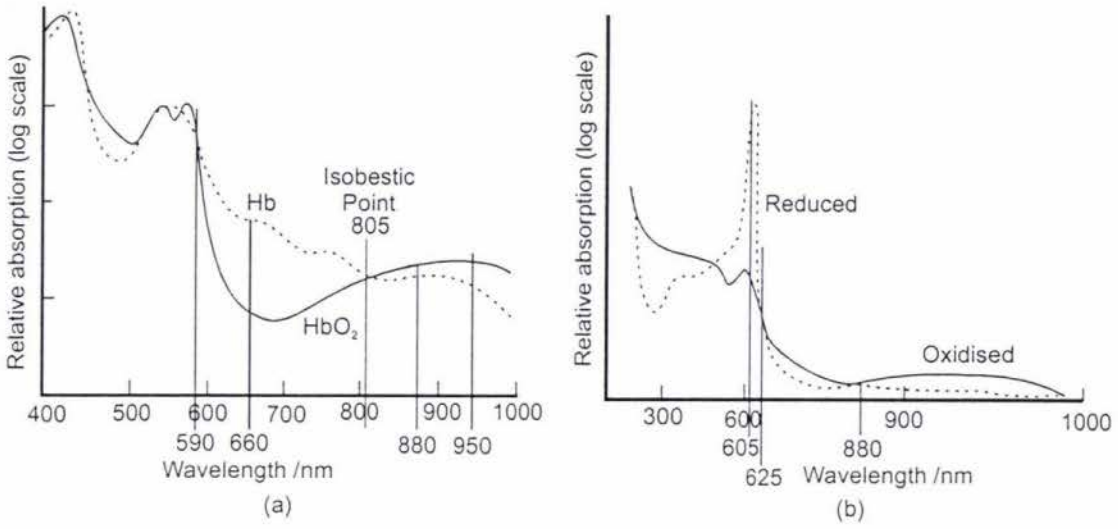

Figure 1.4: (a) Absorption spectra of oxy- and deoxy- haemoglobin and (b) oxidised and reduced cytochrome oxidase [8]. 805nm is the isobestic wavelength for oxy- and deoxy- haemoglobin, other specified wavelengths indicate the frequencies of the available light sources (LEDs).

In radiation transport, light is comprised of discrete photons that are either elastically scattered or totally absorbed according to the coefficients ε (absorption coefficient) and σ (scattering coefficient) for constituents within the tissue [8]. The Beer-Lambert law (1.3) describes the total absorbance as the sum of the absorption coefficients multiplied by the concentration of each absorber [9]. The total absorbance is related to the detected light intensity by the logarithm of the incident and transmitted light (1.4)

$$A = \sum_i \varepsilon_\lambda^{X_i} [X_i] L \tag{1.3}$$

$$A = \log_{10}(I_0 / I) \tag{1.4}$$

where I_0 and I are the intensity of the incident and transmitted light respectfully, $\varepsilon_\lambda^{X_i}$ are the absorption coefficients (at wavelengths λ) for the various absorbers (X_i) in the tissue, $[X_i]$ are the concentration of the absorbers and L is the optical path length. The following result that relates blood oxygen saturation to the measured light intensity is calculated from absorbance data measured at the two wavelengths, 660nm and 880nm. At 660nm, reduced haemoglobin absorbs considerably more than oxyhaemoglobin and at 880nm the absorbance due to oxy- and deoxy- haemoglobin is comparable. The tissue oxygenation result is derived in the same manner using the same assumptions but shorter wavelengths of 605nm and 626nm. The general oxygen saturation derivation using double wavelength measurements is given in appendix A.1.

At 660nm and 880nm it can be assumed that the contribution to the absorption by chromophores other than haemoglobin is small and, on the time scale of an observation, their contribution remains constant [6]. These terms along with optical loss and the sensitivity of the detector can be incorporated into an attenuation constant such that (1.3) may be rewritten as

$$A \propto \left(\varepsilon_\lambda^{Hb}[Hb] + \varepsilon_\lambda^{HbO_2}[HbO_2]\right) L \tag{1.5}$$

Equations (1.4) and (1.5) can be combined resulting in an equation that describes the observed intensity, I, as a function of the optical path length, the oxy- and deoxy-haemoglobin absorption coefficients, and concentrations which vary in a complementary fashion.

In (1.5) the absorbance, A, depends on the optical path length, which is unknown. Work using time-resolved or frequency-domain reflectance spectrometry has been carried out by a number of researchers (Wilson *et al.* [8], Liu *et al.* [10]) to obtain absolute, quantitative absorption data. These techniques however, have large computational and hardware requirements that are unsuitable for this application.

Given the relative transparency of tissue to red and near infrared light it can be assumed that the concentration of scatterers is much greater than the concentration of absorbers and that the degree of scattering varies insignificantly between 660nm and 880nm. That is,

$$(S >> A) \; and \; (S_{660nm} \approx S_{880nm}) \qquad (1.6)$$
$$where \; S = \sum_i \sigma_{X_i} [X_i]$$

Under these conditions, the average optical path length for both wavelengths is approximately equal (i.e. $\langle L_{660nm} \rangle \approx \langle L_{880nm} \rangle$) and, by taking the ratio of absorbances, the optical path length term may be eliminated [8].

$$\frac{A_{660}}{A_{880}} = \frac{\varepsilon_{660}^{Hb}[Hb] + \varepsilon_{660}^{HbO_2}[HbO_2]}{\varepsilon_{880}^{Hb}[Hb] + \varepsilon_{880}^{HbO_2}[HbO_2]} \qquad (1.7)$$

Using the complementary relationship between the oxy- and deoxy- haemoglobin concentration and recalling that the absorbance is proportional to the intensity signal, $A \propto \log(I_0/I)$, an equation that describes the relationship between measured light intensity and oxygen saturation is found (appendix A.1).

$$\frac{[HbO_2]}{[Hb_{total}]} = \frac{\varepsilon_{880}^{Hb} \dfrac{\log(I_{0,660}/I_{660})}{\log(I_{0,880}/I_{880})} - \varepsilon_{660}^{Hb}}{(\varepsilon_{880}^{Hb} - \varepsilon_{880}^{HbO_2}) \dfrac{\log(I_{0,660}/I_{660})}{\log(I_{0,880}/I_{880})} + \varepsilon_{660}^{HbO_2} - \varepsilon_{660}^{Hb}} \qquad (1.8)$$

The reduction state of cytochrome oxidase and measured light intensity is calculated using the same analytical method, however in this case, the difference in absorption is observed for light of wavelength, 605nm (figure 1.4).

From the absorbance relationship (1.5) an equation describing relative blood volume can also be derived by considering the absorbance at two different wavelengths

$$A_{660} \propto \varepsilon_{660}^{Hb}[Hb]L + \varepsilon_{660}^{HbO_2}[HbO_2]L \qquad (1.9)$$
$$A_{880} \propto \varepsilon_{880}^{Hb}[Hb]L + \varepsilon_{880}^{HbO_2}[HbO_2]L \qquad (1.10)$$

Obtaining either (1.9) or (1.10) in terms of $[Hb]$ and $[HbO_2]$ then combining the results gives an equation relating the total haemoglobin concentration to the absorbance (1.11). Assuming that the total haemoglobin concentration in the blood remains approximately constant, the relationship between blood volume and measured light intensity is found by substituting the absorbance relationship, $A \propto \log(I_0/I)$, into (1.11). The general derivation of relative blood volume is given in appendix A.3.

$$[Hb_{total}] \propto \frac{1}{L}\left(\frac{A_{660}\left(\varepsilon_{880}^{HbO_2} - \varepsilon_{880}^{Hb}\right) + A_{880}\left(\varepsilon_{660}^{Hb} - \varepsilon_{660}^{HbO_2}\right)}{\varepsilon_{660}^{Hb}\varepsilon_{880}^{HbO_2} - \varepsilon_{880}^{Hb}\varepsilon_{660}^{HbO_2}} \right) \tag{1.11}$$

1.5.2 TRIPLE WAVELENGTH OXYGEN SATURATION MEASUREMENT

In general, the opacity of tissue reduces for light of increasing wavelength. Within an absorption band (e.g. 590nm to 880nm for oxyhaemoglobin) the background absorbance can be estimated by interpolating between two wavelengths at which the absorbances of the oxidised and reduced states are comparable (figure 1.5). Normalising the acquired absorbance with this predicted reference point reduces the error due to non-uniform base line drift and improves the validity of assumptions made for the constant attenuation assumed in equation (1.5).

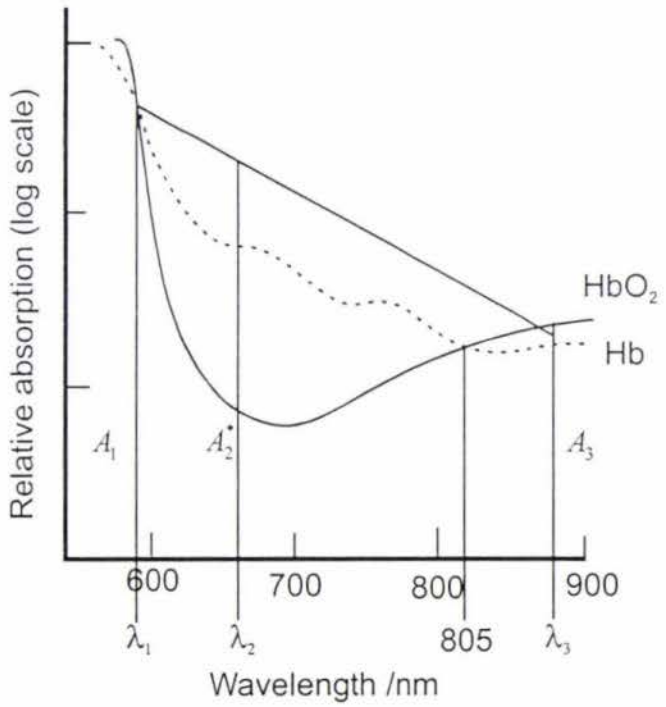

Figure 1.5: Interpolating to find an estimate of the background absorbance at wavelength, λ_2. Comparing the measured absorbance with the background estimate helps to remove the non-uniform baseline drift present in double wavelength measurements.

The equation describing oxygen saturation from triple wavelength measurements is given for the oxygenation state of haemoglobin using the wavelengths λ_1 = 590nm, λ_2 = 660nm and λ_3 = 880nm. A similar result is obtained for cytochrome oxidase

using the wavelengths $\lambda_1 = 590\text{nm}$, $\lambda_2 = 605\text{nm}$ and $\lambda_3 = 625\text{nm}$. The general derivation of triple-wavelength oxygen saturation measurement is given in appendix A.2.

Linearly interpolating between 590nm and 880nm gives an expression for the background absorbance, $A^{\bullet}_{660}$, at 660nm,

$$A^{\bullet}_{660} = \frac{A_{880} - A_{590}}{\Lambda} + A_{590} \qquad (1.12)$$

$$\text{where } \Lambda = \frac{880-590}{660-590} = 4.143$$

Defining, β, as the ratio of the measured absorbance to the background absorbance and assuming again that the mean optical path lengths are approximately equal at all three wavelengths gives the following expression

$$\beta = \frac{A_{660}}{A^{\bullet}_{660}} = \frac{\Lambda\left(\varepsilon^{Hb}_{660}[Hb] + \varepsilon^{HbO_2}_{660}[HbO_2]\right)}{\left(\varepsilon^{Hb}_{880}[Hb] + \varepsilon^{HbO_2}_{880}[HbO_2]\right) + \left(\varepsilon^{Hb}_{590}[Hb] + \varepsilon^{HbO_2}_{590}[HbO_2]\right)(\Lambda - 1)} \qquad (1.13)$$

As before, the complementary relationship between the oxy- and deoxy- haemoglobin concentration is used allowing equation (1.13) to be solved for the oxygen saturation giving,

$$\frac{[HbO_2]}{[Hb_{total}]} = \frac{\beta\left(\varepsilon^{Hb}_{880} + (\Lambda-1)\varepsilon^{Hb}_{590}\right) - \Lambda\varepsilon^{Hb}_{660}}{\Lambda\left(\varepsilon^{HbO_2}_{660} - \varepsilon^{Hb}_{660}\right) + \beta\left[(\Lambda-1)\left(\varepsilon^{Hb}_{590} - \varepsilon^{HbO_2}_{590}\right) + \varepsilon^{Hb}_{880} - \varepsilon^{HbO_2}_{880}\right]} \qquad (1.14)$$

To obtain the direct relationship between measured intensity and oxygen saturation, the absorbance relationship, $A \propto \log(I_0/I)$, is substituted into β

$$\beta = \frac{\Lambda A_{660}}{A_{880} + A_{590}(\Lambda - 1)} = \frac{\Lambda \log\left(I_{0,660}/I_{660}\right)}{\log\left(I_{0,880}/I_{880}\right) + \log\left(I_{0,590}/I_{590}\right)(\Lambda - 1)} \qquad (1.15)$$

In both the double and triple wavelength calculations, relative blood volume, blood oxygenation and tissue oxygenation are found to be functions of the intensity signal and absorption coefficients only. Using data acquired from the device and absorption information from the literature allowed the metabolic state of the subject to be described.

1.5.3 NEAR INFRARED SPECTROMETRY

Near-infrared spectroscopic systems are usually arranged in one of two configurations, transmission mode or reflectance mode (figure 1.6). Established clinical and research devices such as the Wood-Geraci ear-oximeter and the Hewlett-Packard eight-wavelength oximeter are all transmission mode devices [11]. The use of reflectance mode spectrometry was introduced by Brinkman and Zijlystra in 1949 who showed that changes in oxyhaemoglobin saturation could be recorded non-invasively from an

optical sensor attached to the forehead [7]. Reflectance mode oximeters however, have not achieved widespread commercial use due to limited accuracy and difficulties in absolute calibration. For the intended application, absolute calibration of the device was not required, as the main objective was to demonstrate a correlation between environmental conditions and the relative changes in the metabolic response of the Adélie penguin. In this device limitations in accuracy were reduced by the greater intensity of modern LED technology and calculation techniques such as the triple wavelength measurement (section 1.5.2).

Aside from the differences in construction and calibration, the physical basis for both transmission and reflectance mode spectroscopy is the same for measurements of completely diffuse light (i.e. the photon distribution within the medium retains no information about initial direction). Photon diffusion analysis by Kumar and Schmitt [12] has shown that, with a source and detector spacing of greater than 2mm, a collimated incident light source is equivalent to a diffuse source located below the surface in an optically turbid medium such as tissue. Since the Beer-Lambert law describes a measured intensity in terms of the photon path length and the incident light source may be considered diffuse, the detected signal for both transmission and reflectance mode spectroscopy is equivalent.

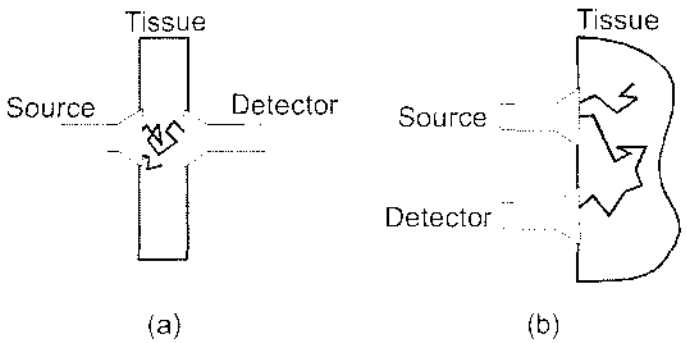

Figure 1.6: The two main configurations for near infrared spectroscopic systems, (a) transmission mode and (b) reflectance mode. For distances greater than 2mm from the incident light source the scattered light may be considered a diffuse light source below the surface. As diffuse light is independent of direction both transmission and reflectance mode spectroscopy are equivalent.

1.6 Thesis Overview

The work undertaken in this thesis involves the design and development of a NIR spectroscopic device. Using the principles and techniques described above, a system was developed that not only collected the necessary physiological data but also addressed some of the difficulties of working in Antarctica and with the Adélie penguin. In the instrumentation chapter that follows, the hardware is assembled along with justification for the components selected. A logical division between measurement and control exists that divides the hardware into analogue and digital stages respectively. The acquired signal is followed through the various analogue processes to the point of digitisation where focus is then moved to the control of the device by the digital components.

The third chapter examines the control of the device from a software perspective. It gives a description of the operating system and the interaction between measurement sequence files, the terminal emulation software and the embedded processor. The final section of this chapter describes the algorithm used to determine pulse rate from the fluctuating scattered light signal and gives analysis of the signal processing techniques used to overcome noise.

Chapter four begins by describing the incremental development of the device and the results of the validation steps taken at each stage. Reasons for each new prototype and the increased functionality that each system allowed are described in the logical order in which they were developed and the conclusion to this section gives the test results of the final prototype version of the device. The second part of chapter four describes the results obtained during field-testing. Included are the physical aspects of the experiments, such as capture, attachment and behavioural response, through to the biological results obtained in response to stress and temperature changes: oxyhaemoglobin saturation, cytochrome oxidase saturation, blood volume and pulse rate. A discussion of the acquired data follows in the conclusion chapter that then lead to an evaluation of the device, its limitations and various suggested improvements. Long-term enhancements conclude chapter five with an outlook toward the potential future of the device in environments as equally diverse as that of the Adélie penguin.